Wavelet based comparison of high frequency oscillations in the geodetic and fluid excitation functions of polar motion

Wiesław Kosek [1,2], Waldemar Popiński [1], Tomasz Niedzielski [1,3]

1) Space Research Centre of the Polish Academy of Sciences,
2) Environmental Engineering and Land Surveying, University of Krakow
3) Oceanlab, University of Aberdeen, Scotland, UK

Journées 2010 "Systèmes de référence spatio-temporels" 20-22 September 2010, Paris

MOTIVATION

- Seasonal and shorter period oscillations of polar motion are wide band oscillations which are mostly driven by equatorial components of the fluid excitation functions.
- Wavelet based techniques enable time–frequency comparison between the geodetic (computed from pole coordinates data) and fluid excitation functions.
- Such an analysis would be very helpful for EOP forecasting purposes if a prediction technique used fluid excitation functions as input data.

DATA

- Equatorial components of the effective angular momentum functions (AAM, OAM and HAM) from ECMWF atmospheric data produced by IERS Associated Product Centre Deutsches GeoForschungsZentrum Potsdam in Jan. 1st 1989 – Dec. 31st 2009 (Dill 2008, Dobslaw and Thomas 2007)

- IERS pole coordinates data x, y *EOPC04_IAU2000.62-now* in 1962 – 2010, http://hpiers.obspm.fr/iers/eop/eopc04_05/

  Geodetic excitation functions ψ were computed from the IERSC04 pole coordinates data using the time domain Wilson and Haubrich (1976) deconvolution formula.

x, y pole coordinates model data computed from fluid excitation functions

Differential equation of polar motion:

$$\frac{i}{\sigma_{ch}}\dot{m}(t)+m(t)=\chi(t)$$

$m(t)=x(t)-iy(t)$ - pole coordinates model data,

$\chi(t)=\chi_1(t)+i\chi_2(t)$ - equatorial excitation functions (AAM, OAM, HAM) or their combinations (AAM+OAM, AAM+OAM+HAM)

$\sigma_{ch}=\frac{2\pi}{T_{ch}}\left(1+\frac{i}{2Q}\right)$ - complex-valued Chandler frequency, where $T_{ch}=433$ *days* and $Q=170$ is the quality factor

Approximate solution of this equation in discrete time moments can be obtained using the trapezoidal rule of numerical integration:

$$m(t+\Delta t)=m(t)\cdot\exp\left(i\sigma_{ch}\Delta t\right)-i\frac{\sigma_{ch}\Delta t}{2}\left[\chi(t+\Delta t)+\chi(t)\cdot\exp\left(i\sigma_{ch}\Delta t\right)\right]$$

x, y pole coordinates model data computed from fluid excitation functions

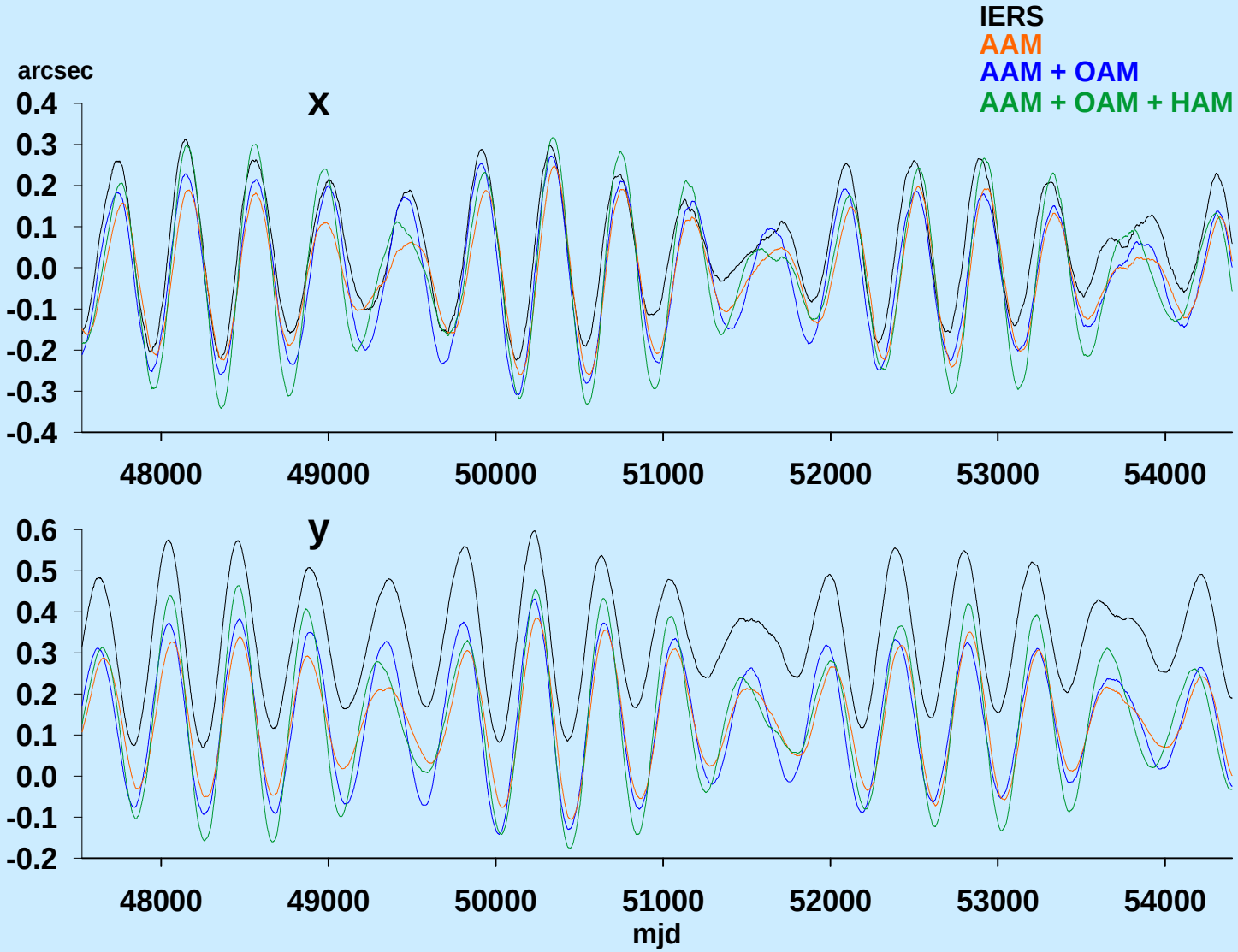

THE MORLET WAVELET TRANSFORM SEMBLANCE

The wavelet transform coefficients of complex-valued signal $x(t)$:

$$X(b,a)=\frac{1}{2\pi}|a|^{1/2}\int_{-\infty}^{\infty}\breve{x}(\omega)\overline{\breve{\varphi}}(a\omega)\exp(ib\omega)d\omega,$$

$CFT[x(t)]$ $\quad$ $CFT[\varphi(t)]$

$a\neq 0$ - dilation,
b - translation

$\varphi(t)\approx\exp(-t^2/2)\exp(i2\pi\cdot t)/\sqrt{2\pi}$ - Morlet wavelet function

The spectro-temporal semblance of the order r between $x(t)$ and $y(t)$ time series:

$$\hat{\vartheta}^r_{xy}(t,a)=\frac{\left|\hat{S}_{xy}(t,a)\right|}{\sqrt{\hat{S}_{xx}(t,a)\hat{S}_{yy}(t,a)}}\cdot\cos^r(\Delta\hat{\phi}_{xy}(t,a)),\qquad t=m_o+m/2,\qquad m_o=0,1,\ldots,n-1-m,\qquad r=1,3,5\ldots$$

$\hat{\kappa}_{xy}(t,a)$
coherence

$$\Delta\hat{\phi}_{xy}(t,a)=\arg\left\{\frac{1}{m}\sum_{b=m_o}^{m_o+m}[\hat{X}(t+b,a)\overline{\hat{Y}(t+b,a)}]/\left|\hat{X}(t+b,a)\right|\left|\hat{Y}(t+b,a)\right|\right\}$$

phase synchronization

$$\hat{S}_{xx}(t,a)=\sum_{b=m_o}^{m_o+m}\left|\hat{X}(t+b,a)\right|^2/m,$$

$$\hat{S}_{yy}(t,a)=\sum_{b=m_o}^{m_o+m}\left|\hat{Y}(t+b,a)\right|^2/m,$$

spectra of $x(t)$, $y(t)$

$\hat{S}_{xy}(t,a)=\sum_{b=m_o}^{m_o+m}\hat{X}(t+b,a)\overline{\hat{Y}(t+b,a)}/m$ - cross-spectrum between $x(t)$ and $y(t)$

The spectro-temporal coherence (semblance, order=0) between the geodetic and fluid excitation functions: *AAM*, *AAM+OAM* and *AAM+OAM+HAM*

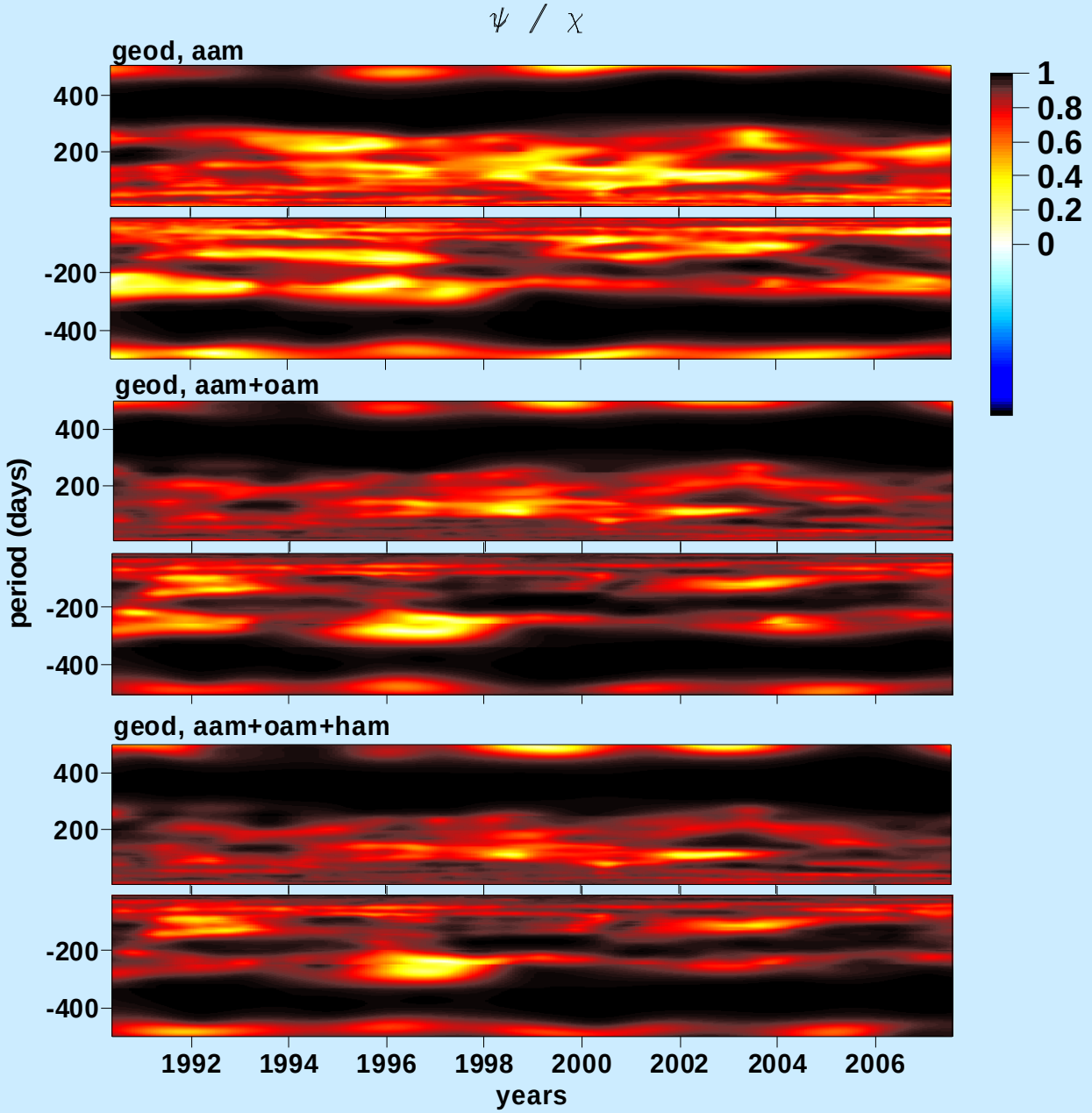

The spectro-temporal semblance (order=3) between the geodetic and fluid excitation functions *AAM*, *AAM+OAM* and *AAM+OAM+HAM*

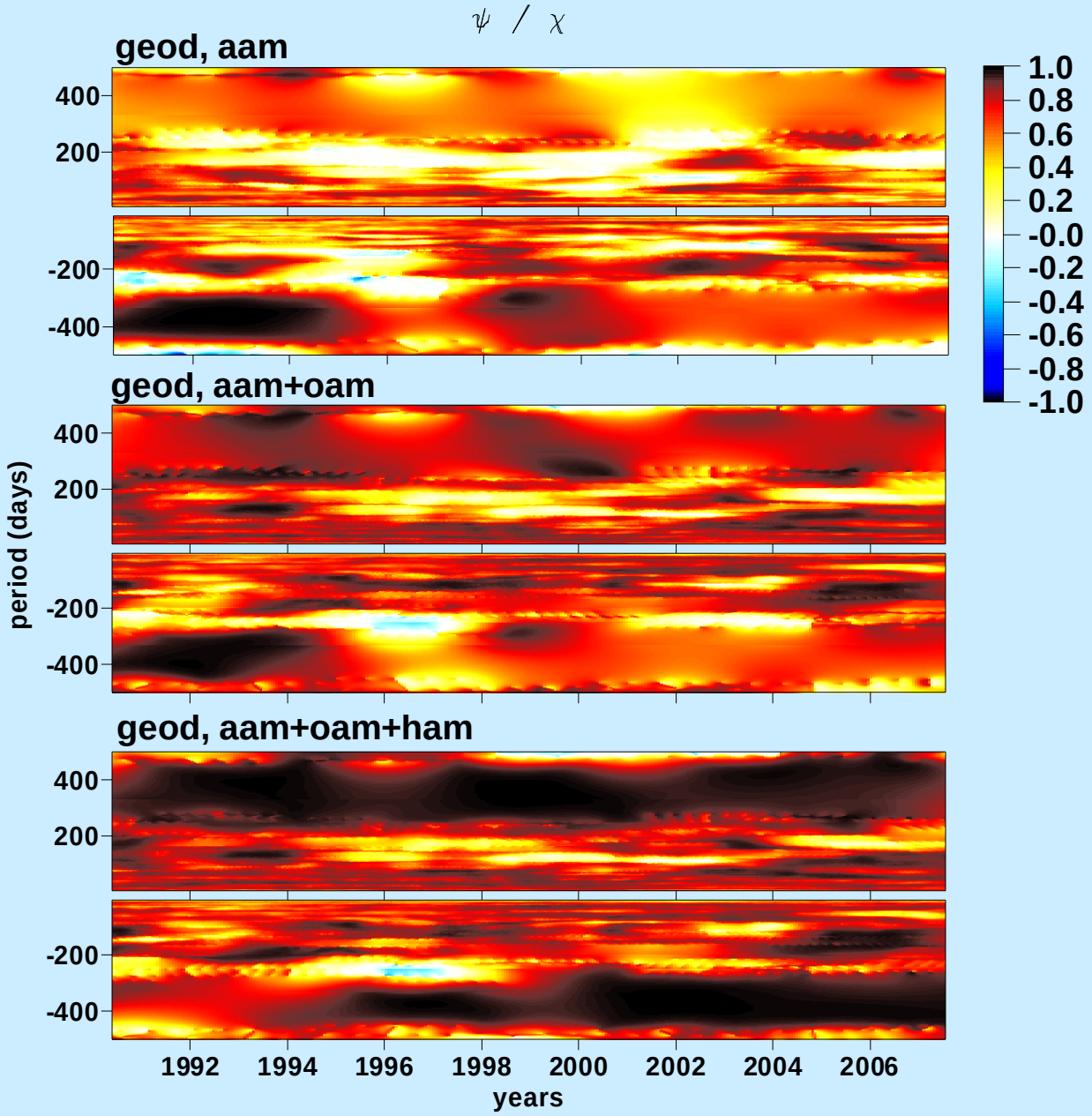

The semblance (order 0, 1 and 3) between the geodetic and fluid excitation functions *AAM*, *AAM+OAM* and *AAM+OAM+HAM*

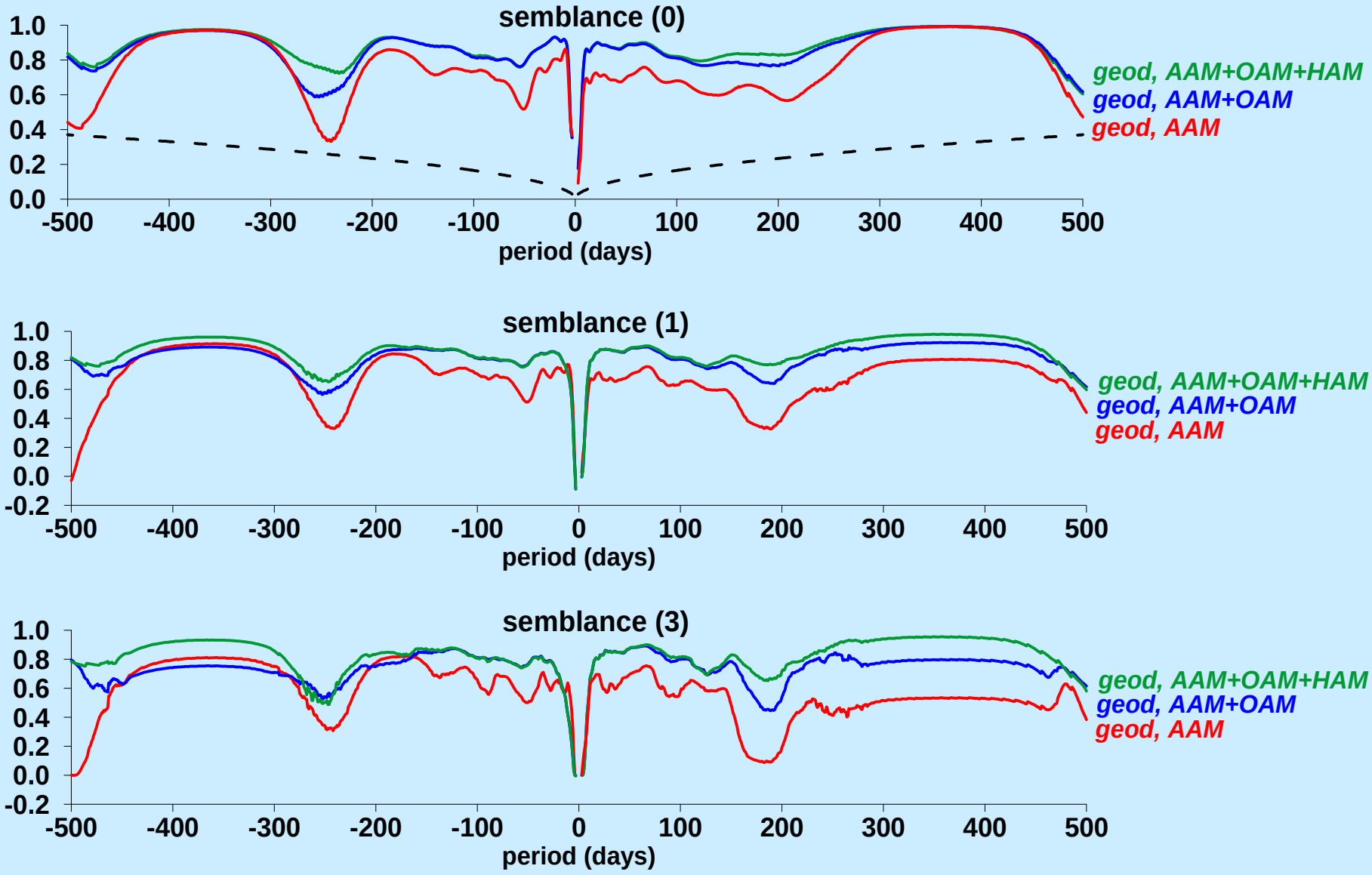

THE WAVELET TRANSFORM POLARIZATION

$$\hat{p}_{XX}(t,|a|)=\frac{\hat{S}_{xx}(t,|a|)-\hat{S}_{xx}(t,-|a|)}{\hat{S}_{xx}(t,|a|)+\hat{S}_{xx}(t,-|a|)},$$

$\hat{S}_{xx}(t,a)=\sum_{b=m_o}^{m_o+m}\left|\hat{X}(t+b,a)\right|^2/m$ - wavelet spectrum

retrograde | **prograde**

$\hat{p}_{XX}(t,|a|)=-1$ $\quad -1<\hat{p}_{XX}(t,|a|)<0$ $\quad 0<\hat{p}_{XX}(t,|a|)<1$ $\quad \hat{p}_{XX}(t,|a|)=1$

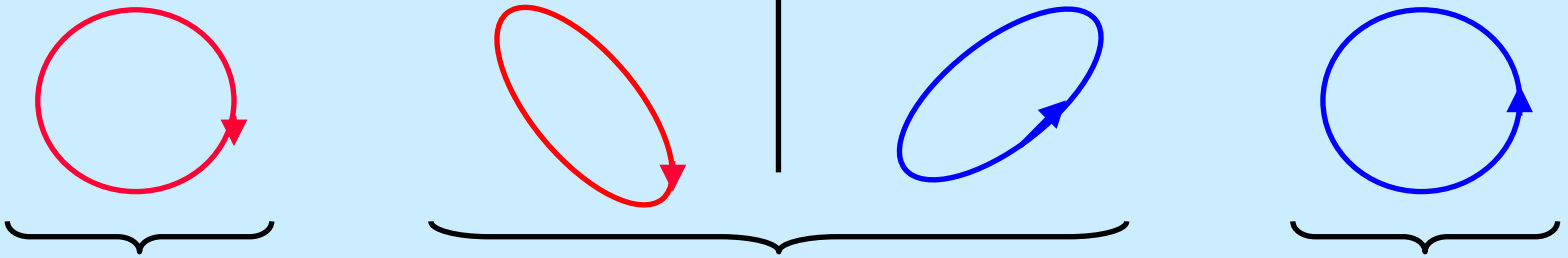

circular $\quad$ **elliptic** $\quad$ **circular**

the shape of ellipse degenerates to a line

$$\hat{p}_{XX}(t,|a|)=0$$

The spectro-temporal polarization functions of the geodetic and fluid AAM, AAM+OAM and AAM+OAM+HAM excitation functions

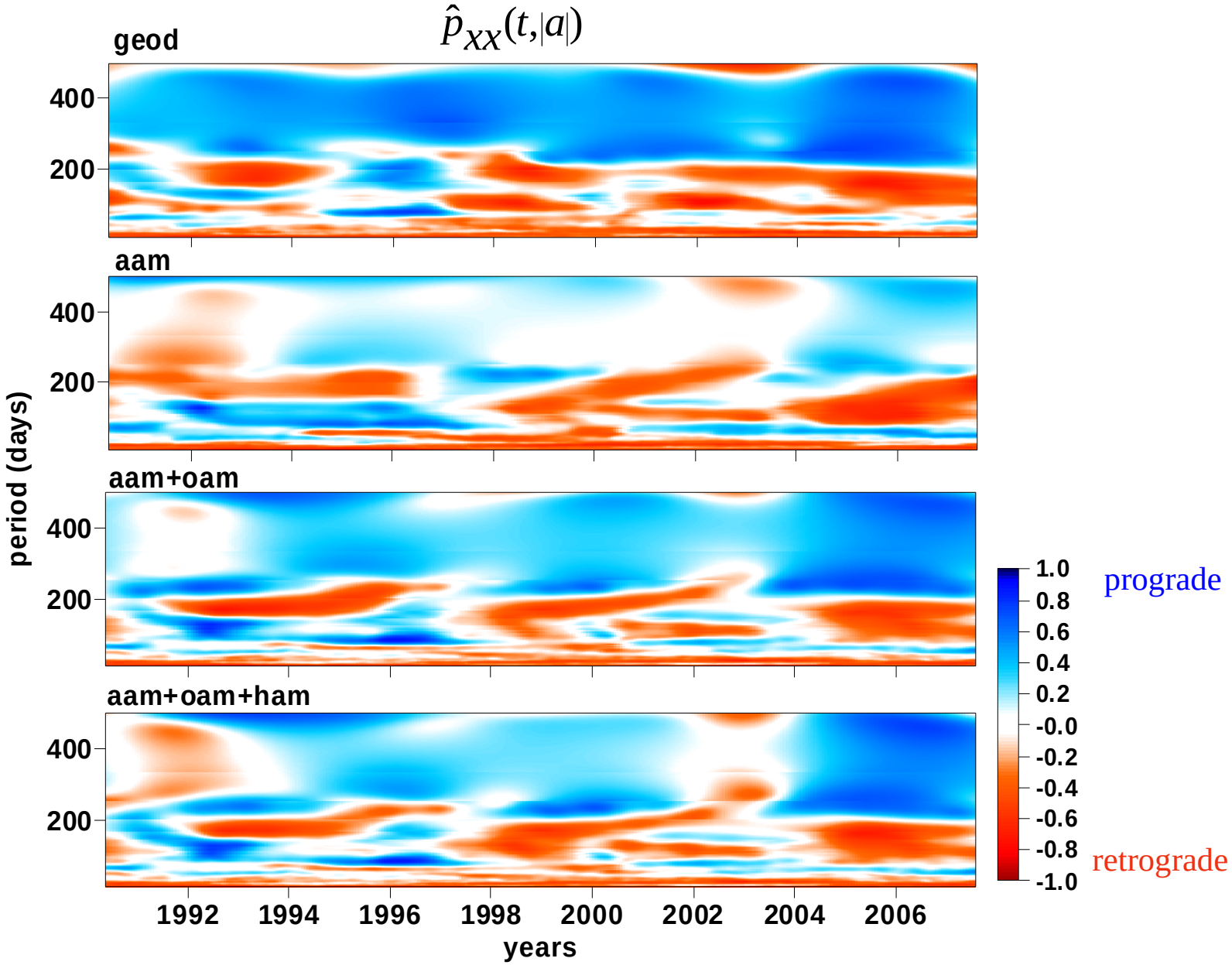

The spectro-temporal polarization functions of x, y IERS pole coordinates data and the model pole coordinates data computed from fluid AAM, AAM+OAM and AAM+OAM+HAM excitation functions

$$\hat{p}_{xx}(t,|a|)$$

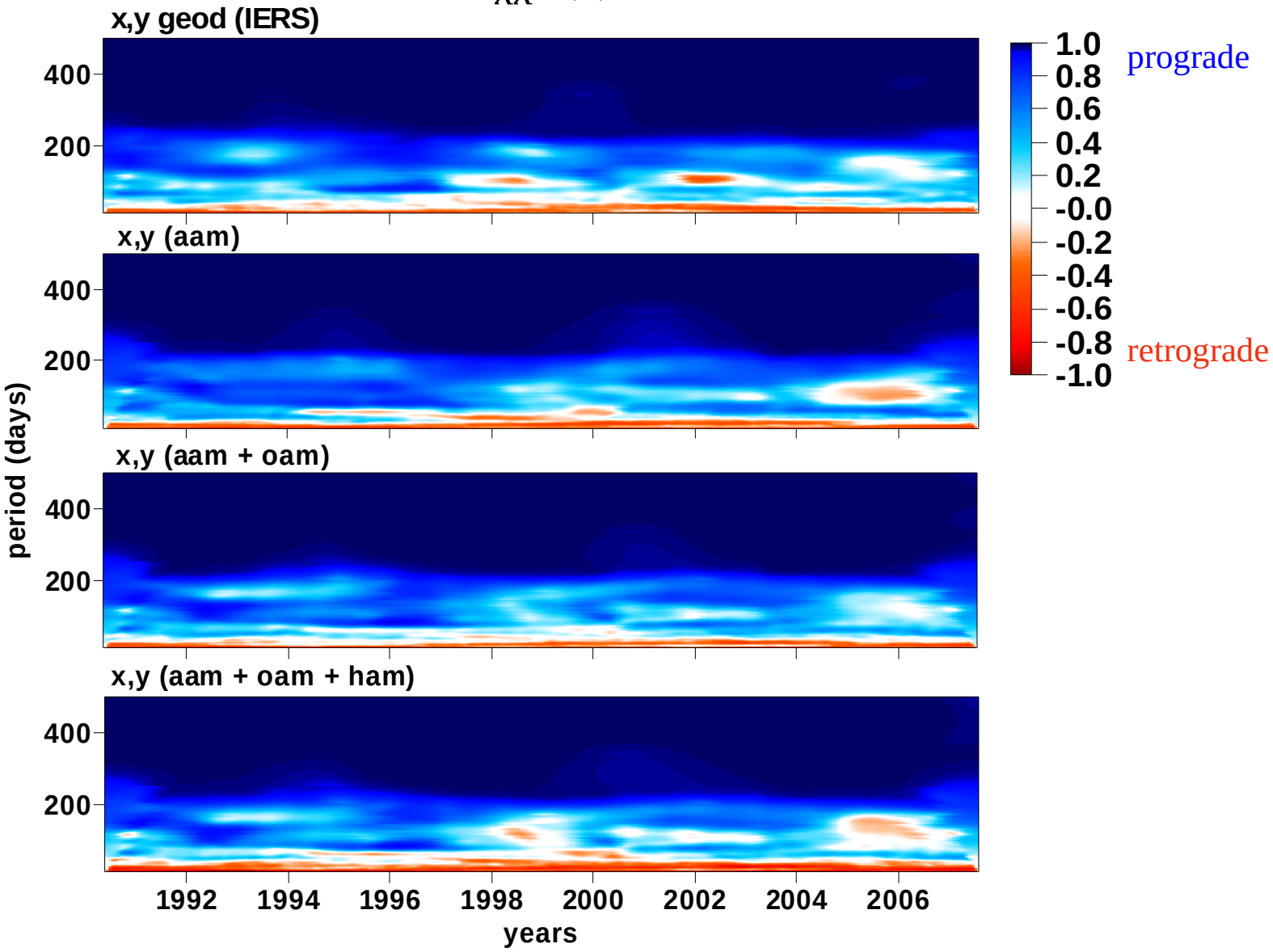

The mean polarization functions of :

a) the geodetic (black) and fluid: AAM, AAM+OAM, AAM+OAM+HAM excitation functions

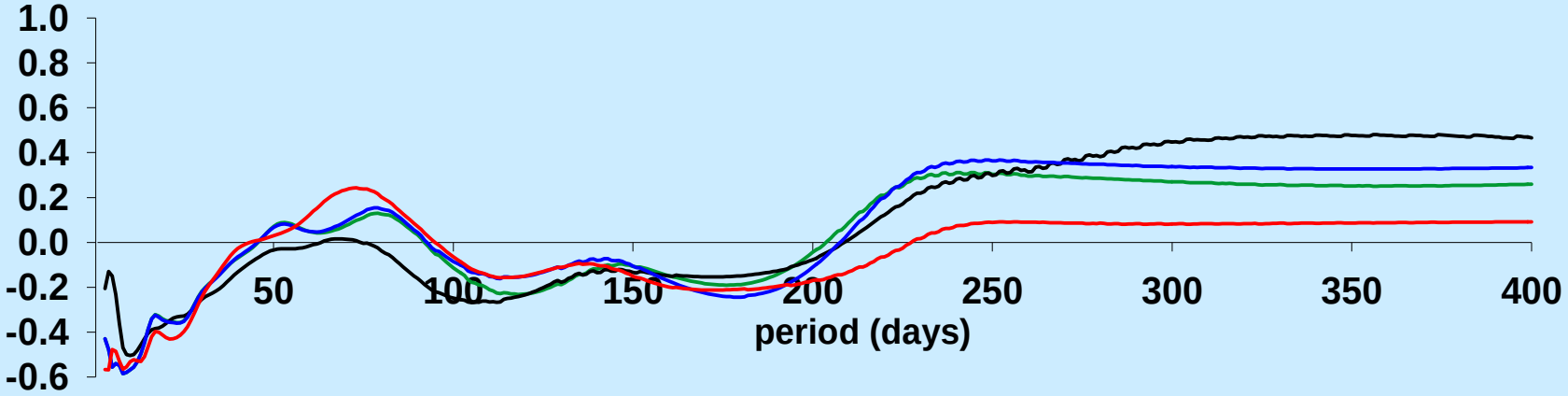

b) the IERS pole coordinates data (black) and the pole coordinates model data computed from AAM, AAM+OAM and AAM+OAM+HAM excitation functions

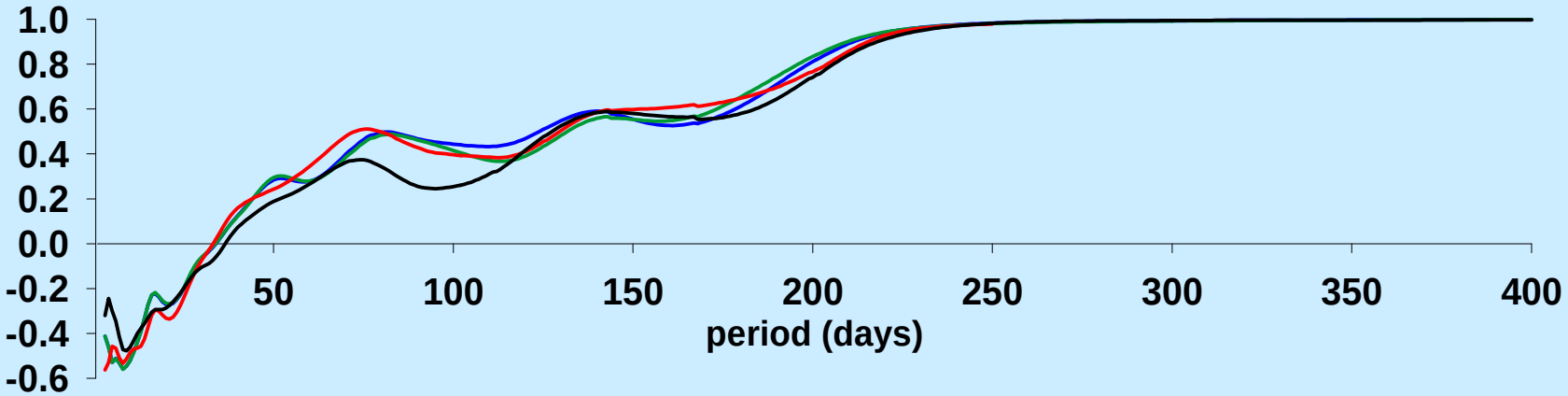

Wavelet based semblance filtering

Wavelet semblance function of two discrete complex-valued signals $x(t), y(t), \quad t = 0,1,\ldots,n-1, \quad n = 2^p$ **is defined for scale index** j **and translation index** k **as**

$$\vartheta_{j,k}^{xy} = \cos(\theta) = \Re e\left\{ \frac{S_{j,k}^{x}\,\overline{S}_{j,k}^{y}}{\left|S_{j,k}^{x}\right|\left|S_{j,k}^{y}\right|} \right\}$$

where:

$S_{j,k}^{x} = \sum_{t=0}^{n-1} x(t)\overline{\varphi}_{j,k}(t), \quad S_{j,k}^{y} = \sum_{t=0}^{n-1} y(t)\overline{\varphi}_{j,k}(t)$ **are the wavelet transform coefficients of** $x(t), y(t)$

θ **is interpreted as the angle between** $S_{j,k}^{x}$, $S_{j,k}^{y}$ **in the complex plane**

$\varphi_{j,k}(t)$ **is the discrete Shannon wavelet function**

The semblance function varies in the interval <-1,1> and shows oscillations in two time series out of phase (-1) and in phase (1).

Discrete Shannon wavelet functions

For the fixed lowest frequency index , $j_0 = 0,1,\ldots, p-2$ **and the corresponding time translation indices** $k = -2^{j_0}, -2^{j_0}+1, \ldots, 2^{j_0}-1$**, the discrete Shannon wavelets are defined by:**

$$\varphi_{j_0}(t) = \frac{1}{n}\exp[-i\pi(t-n/2)/n]\frac{\sin[2^{j_0+1}\pi(t-n/2)/n]}{\sin[\pi(t-n/2)/n]}, \qquad \varphi_{j_0}(n/2) = 2^{j_0+1}/n,$$

$$\varphi_{j_0,k}(t) = \sqrt{n}2^{-\frac{(j_0+1)}{2}}\varphi_{j_0}(t-n/2-2^{-(j_0+1)}kn)$$

For higher frequency indices $j = j_0+1, j_0+2, \ldots, p-1,$ **and corresponding time translation indices** $k = -2^{j-1}, -2^{j-1}+1, \ldots, 2^{j-1}-1$ **, the discrete Shannon wavelets are defined by:**

$$\varphi_j(t) = \frac{1}{n}\exp[-i\pi(t-n/2)/n]\frac{\sin[2^j\pi(t-n/2)/n](2\cos[2^j\pi(t-n/2)/n]-1)}{\sin[\pi(t-n/2)/n]},$$

$$\varphi_j(n/2) = 2^j/n, \qquad \varphi_{j,k}(t) = \sqrt{n}2^{-j/2}\varphi_j(t-n/2-2^{-j}kn)$$

The reconstruction formula of $x(t)$ **time series is given by:**

$$\sum_{j=j_0}^{p-1}\sum_{k=-2^{j-1}}^{2^{j-1}-1} S_{j,k}^{x}\varphi_{j,k}(t) = x(t) \qquad for \qquad t = 0,1,\ldots,n-1.$$

Semblance filtering is performed by keeping in the reconstruction formulae of both time series

$$\sum_{j=j_0}^{p-1}\sum_{k=-2^{j-1}}^{2^{j-1}-1} S_{j,k}^{x}\varphi_{j,k}(t)=x(t), \quad \sum_{j=j_0}^{p-1}\sum_{k=-2^{j-1}}^{2^{j-1}-1} S_{j,k}^{y}\varphi_{j,k}(t)=y(t)$$

only the wavelet transform coefficients $\tilde{S}_{j,k}^{x},\tilde{S}_{j,k}^{y}$ **for which the semblance** $\vartheta_{j,k}^{xy}$ **exceeds a given threshold equal to 0.90 or 0.99. Other wavelet transform coefficients of both time series, for which the semblance was below the adopted threshold, were set to zero.**

The common signals in $x(t)$ **and** $y(t)$ **can be computed using the following reconstruction formula:**

$$x_{sf}(t)=\sum_{j=j_0}^{p-1}\sum_{k=-2^{j-1}}^{2^{j-1}-1} \tilde{S}_{j,k}^{x}\varphi_{j,k}(t), \quad y_{sf}(t)=\sum_{j=j_0}^{p-1}\sum_{k=-2^{j-1}}^{2^{j-1}-1} \tilde{S}_{j,k}^{y}\varphi_{j,k}(t)$$

Using semblance filtering with the discrete Shannon wavelet functions it's possible to filter from both time series variations characterized by a good phase agreement. It enables computation of common oscillations in all possible frequency bands in two complex-valued time series.

The common oscillations in the equatorial components of geodetic (black) and AAM, OAM and HAM excitation functions, computed using wavelet based semblance filtering (threshold = 0.9).

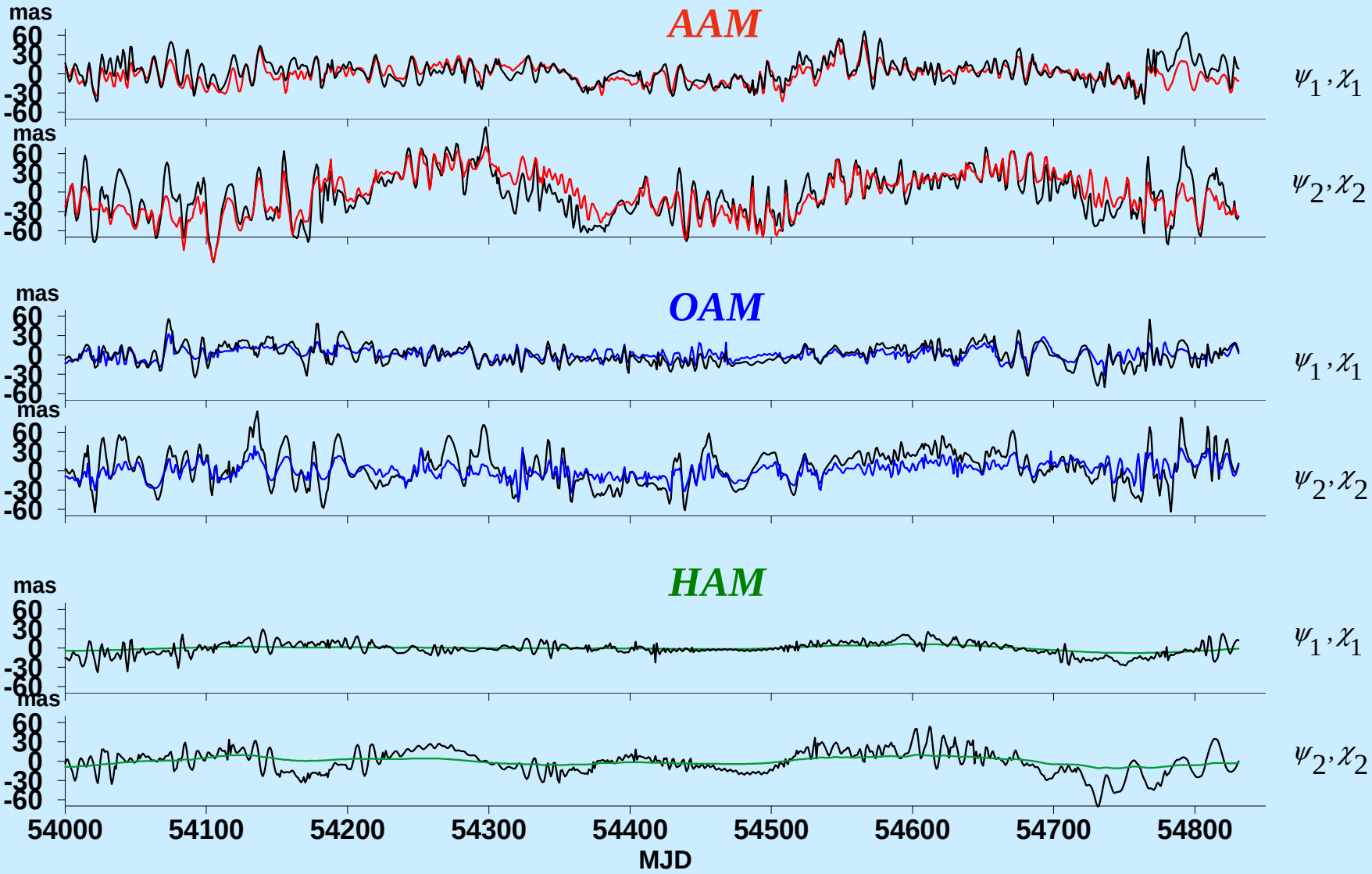

The common oscillations in the equatorial components of geodetic (black) and AAM+OAM+HAM (brown) excitation functions, computed using wavelet based semblance filtering (threshold values equal to 0.90 and 0.99).

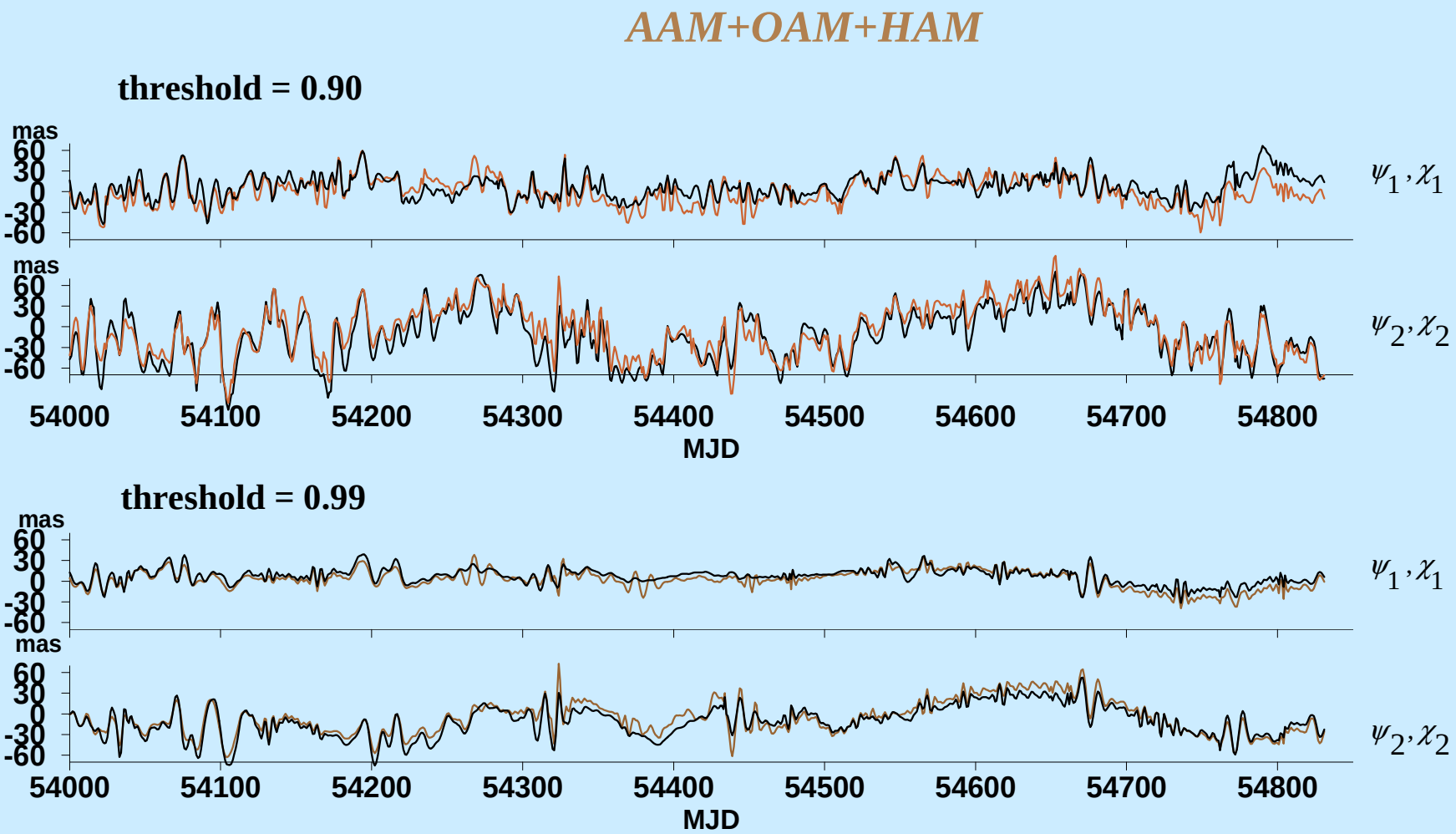

Table 1. Correlation coefficients in 1989.0-2009.0 between the geodetic ψ_1,ψ_2 and fluid χ_1,χ_2 excitation functions, computed using wavelet based semblance filtering for threshold values equal to 0.00, 0.90 and 0.99.

threshold	**0.00**		**0.90**		**0.99**	
Fluid excitation	ψ_1/χ_1	ψ_2/χ_2	ψ_1/χ_1	ψ_2/χ_2	ψ_1/χ_1	ψ_2/χ_2
AAM	**0.441**	**0.642**	**0.773**	**0.856**	**0.828**	**0.866**
AAM+OAM	**0.553**	**0.710**	**0.823**	**0.895**	**0.868**	**0.924**
AAM+OAM+HAM	**0.562**	**0.728**	**0.830**	**0.909**	**0.883**	**0.926**

CONCLUSIONS

- **Wavelet based techniques enable time-frequency comparison of the geodetic and fluid excitation functions.**
- **The oscillations in pole coordinates data or pole coordinates model data computed from fluid excitation functions with periods greater than ~230 days are prograde and almost circular. For shorter period oscillations are still prograde but become more elliptic, and for oscillations with periods less than ~35 days they become more retrograde than prograde.**
- **Higher order semblance function reveals that addition of hydrology angular momentum to the sum of atmospheric and oceanic ones improves the phase agreement between the geodetic and fluid excitation functions in the annual frequency band.**
- **The common oscillations in the geodetic and fluid excitation functions can be detected using wavelet based semblance filtering.**

Thank You

References:

Cooper G.R.J. and D.R. Cowan, 2008, Comparing time series using wavelet-based semblance analysis, ***Computers & Geosciences*** 34 (2008) 95–102.

Cooper G.R.J. 2009, Wavelet based semblance filtering, ***Computers and Geosciences*** 35, pp. 1988-1991.

Dill R. 2008, Hydrological model LSDM for operational Earth rotation and gravity field variations. ***Scientific Technical Report*** STR08/09, GFZ, Potsdam, Germany, 35p.

Dobslaw H., Thomas M. 2007, Simulation and observation of global ocean mass anomalies. ***J. Geophys. Res.***, 112, C05040, doi:10.1029/2006JC004035.

Frazier M. and Torres R. 1994, The sampling theorem, S-transform, and Shannon wavelets for *R,Z,T* and *ZN*, in Benedetto J.J., Frazier M.W., eds, ***Wavelets- Mathematics and Applications***, CRC Press, Boca Raton, pp. 221-245.

Acknowlegements. This paper was supported by the Polish Ministry of Science and Education, project N N526160136 under the leadership of Dr. T. Niedzielski

presentation available: http://www.cbk.waw.pl/~kosek

The difference of spectro-temporal polarization functions between the geodetic and fluid AAM, AAM+OAM, AAM+OAM+HAM excitation functions

$$\left[\hat{p}_{xx}(t,|a|) - \hat{p}_{yy}(t,|a|)\right]/2$$

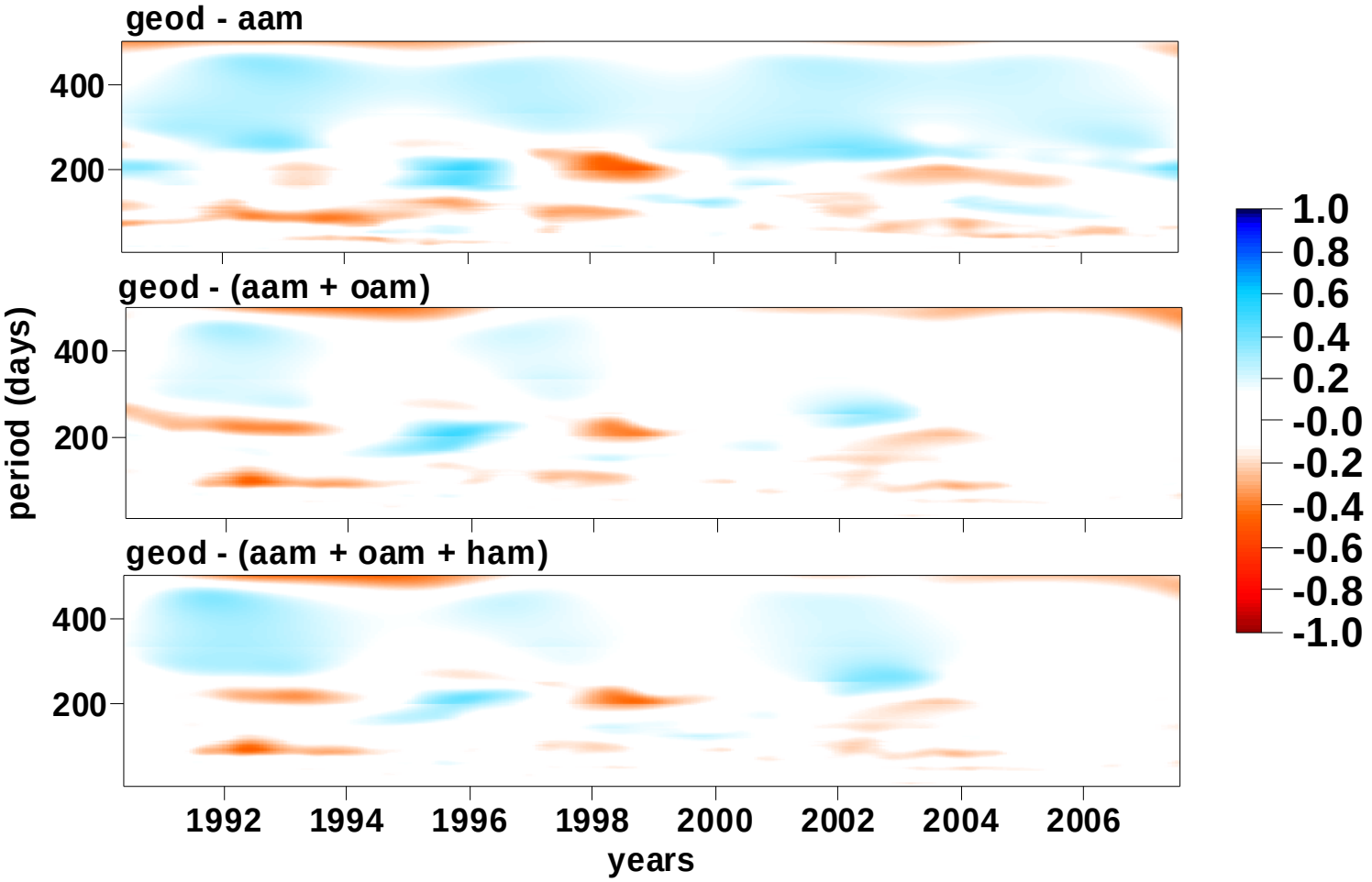

The difference of spectro-temporal polarization functions between x, y IERS pole coordinates data and the model pole coordinates data computed from fluid: AAM, AAM+OAM and AAM+OAM+HAM excitation functions

$$\left[\hat{p}_{xx}(t,|a|)-\hat{p}_{yy}(t,|a|)\right]/2$$

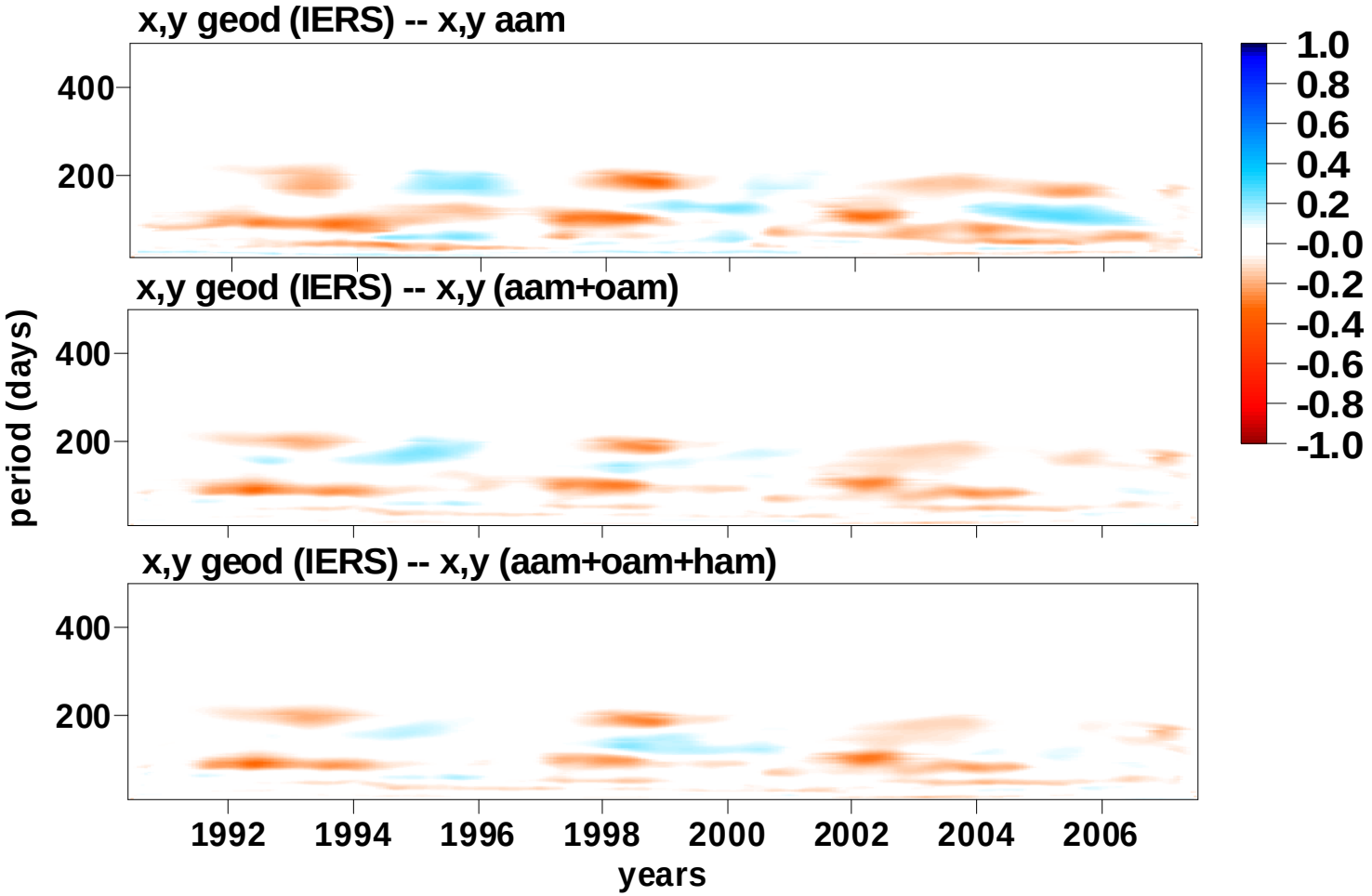

The MWT frequency dependent cross-covariance functions (σ=1.0) between the geodetic and fluid: *AAM* or *AAM+OAM* or *AAM+OAM+HAM* excitation functions and the corresponding frequency dependent time lag functions

$$\hat{S}_{xy}(t,a)=\sum_{b=m_o}^{m_o+m}\hat{X}(t+b,a)\overline{\hat{Y}(t+b,a)}/m$$

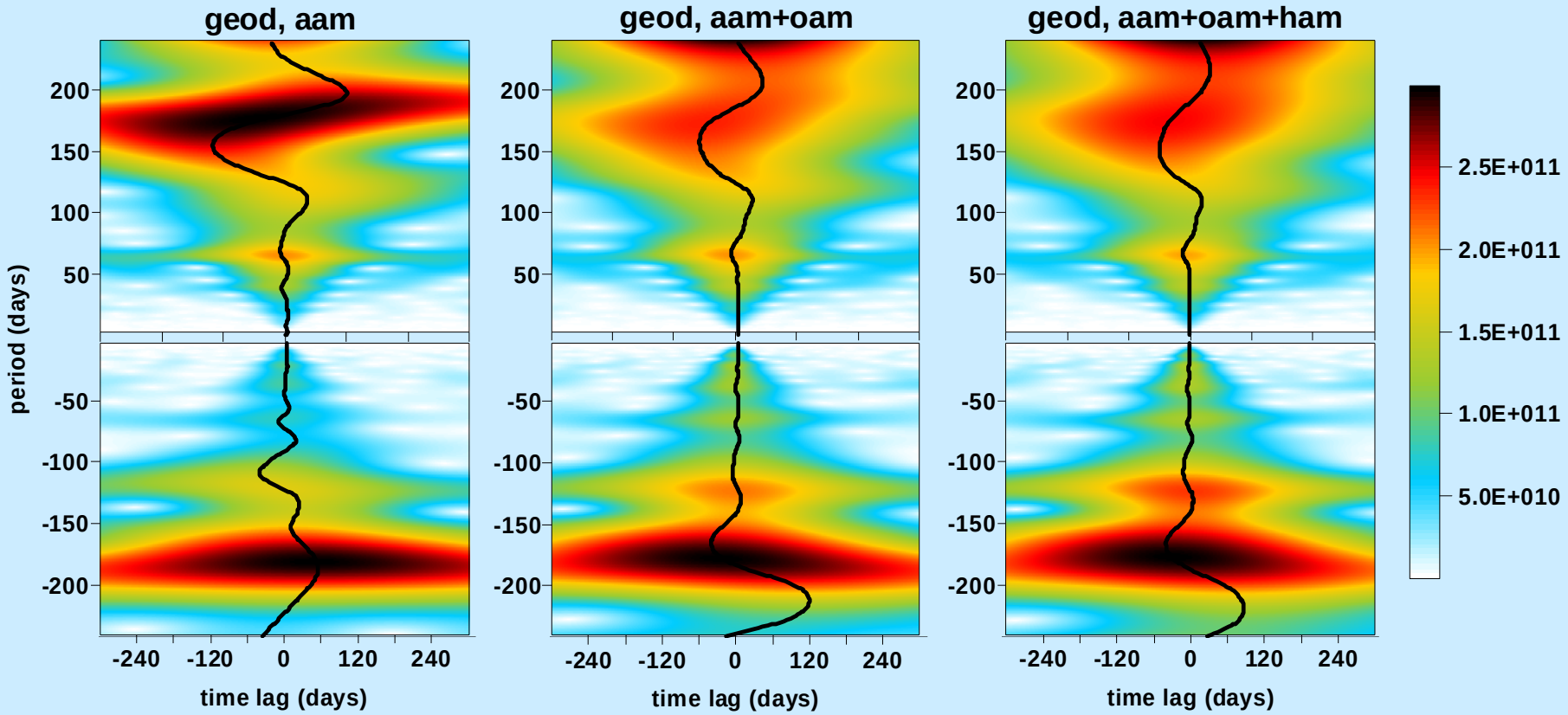

The MWT frequency dependent cross-covariance functions (σ=0.7) between the geodetic and fluid: *AAM* or *AAM+OAM* or *AAM+OAM+HAM* excitation functions and the corresponding frequency dependent time lag functions

$$\hat{S}_{xy}(t,a)=\sum_{b=m_o}^{m_o+m}\hat{X}(t+b,a)\overline{\hat{Y}(t+b,a)}/m$$

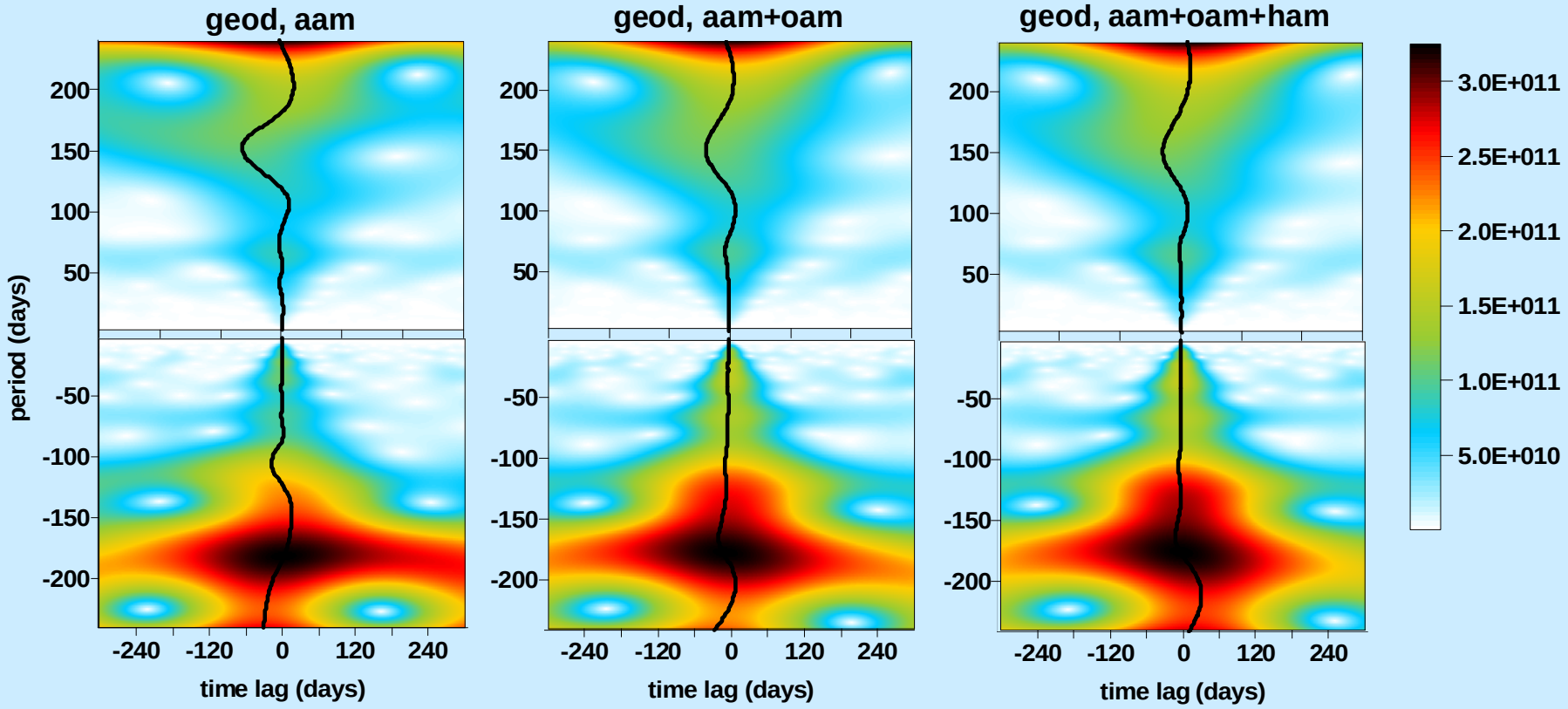

The DWT frequency components of *x* pole coordinate data

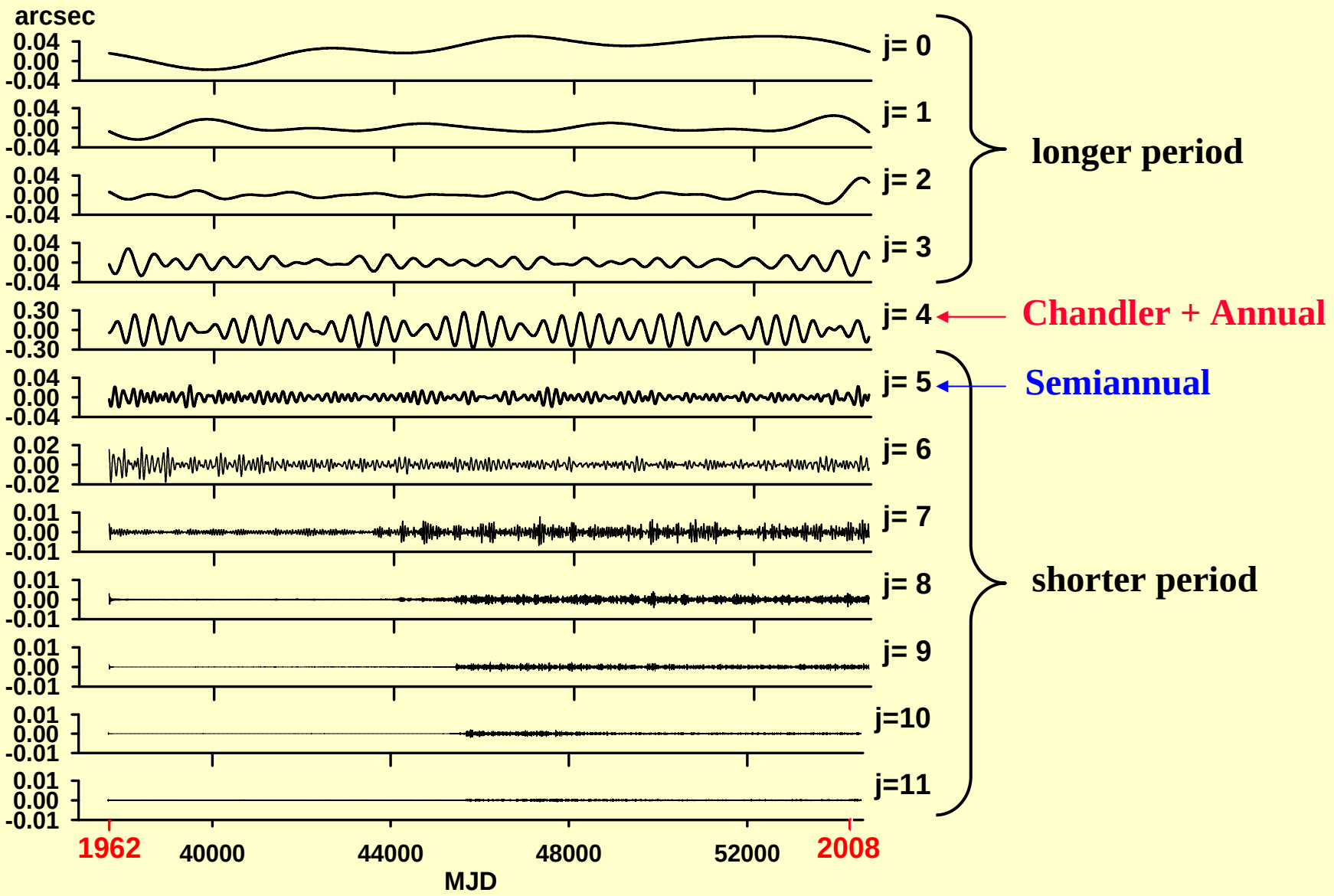

Table 1. Correlation coefficients in 1989.0-2009.0 between the geodetic ψ_1,ψ_2 and fluid χ_1,χ_2 excitation functions, computed using wavelet based semblance filtering for threshold values equal to 0.00, 0.90 and 0.99.

threshold	0.00		0.90		0.99	
Fluid excitation	ψ_1/χ_1	ψ_2/χ_2	ψ_1/χ_1	ψ_2/χ_2	ψ_1/χ_1	ψ_2/χ_2
AAM	0.441	0.642	0.773	0.856	0.828	0.866
OAM	0.336	0.313	0.779	0.792	0.788	0.816
HAM	0.114	0.093	0.476	0.585	0.583	0.751
AAM+OAM	0.553	0.710	0.823	0.895	0.868	0.924
AAM+HAM	0.440	0.684	0.706	0.866	0.856	0.883
OAM+HAM	0.361	0.302	0.806	0.815	0.860	0.857
AAM+OAM+HAM	0.562	0.728	0.830	0.909	0.883	0.926

Amplitudes and phases of the most energetic oscillations in x, y pole coordinates data

Amplitudes

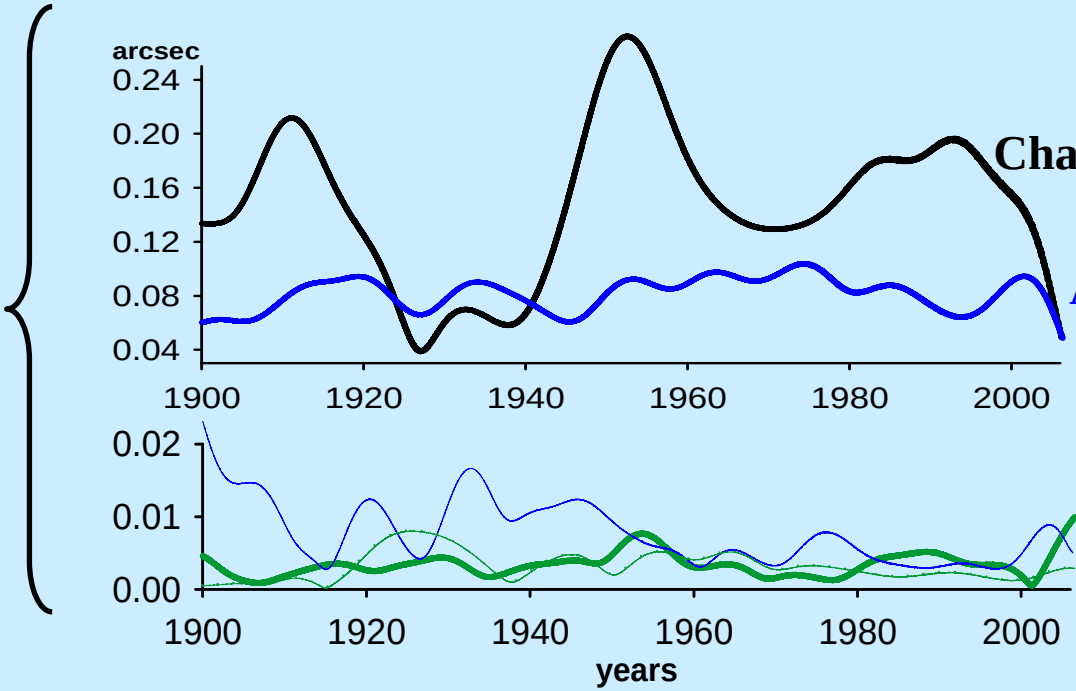

bold line – prograde
thin line - retrograde

Phases

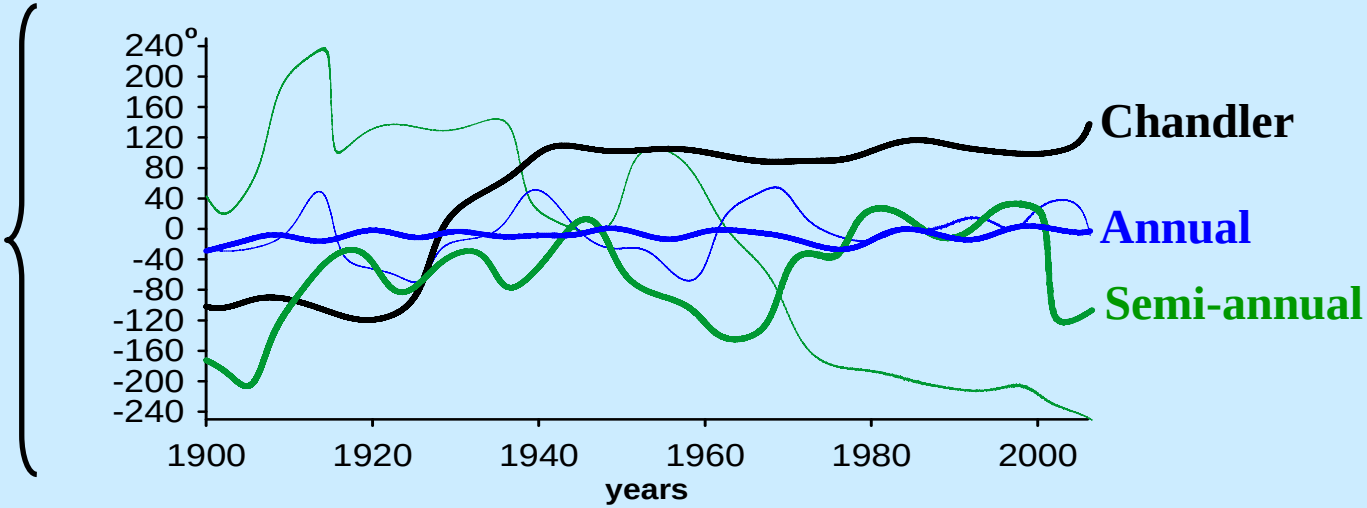

The MWT spectro-temporal semblance (order=1) between the geodetic and fluid excitation functions *AAM*, *AAM+OAM* and *AAM+OAM+HAM*

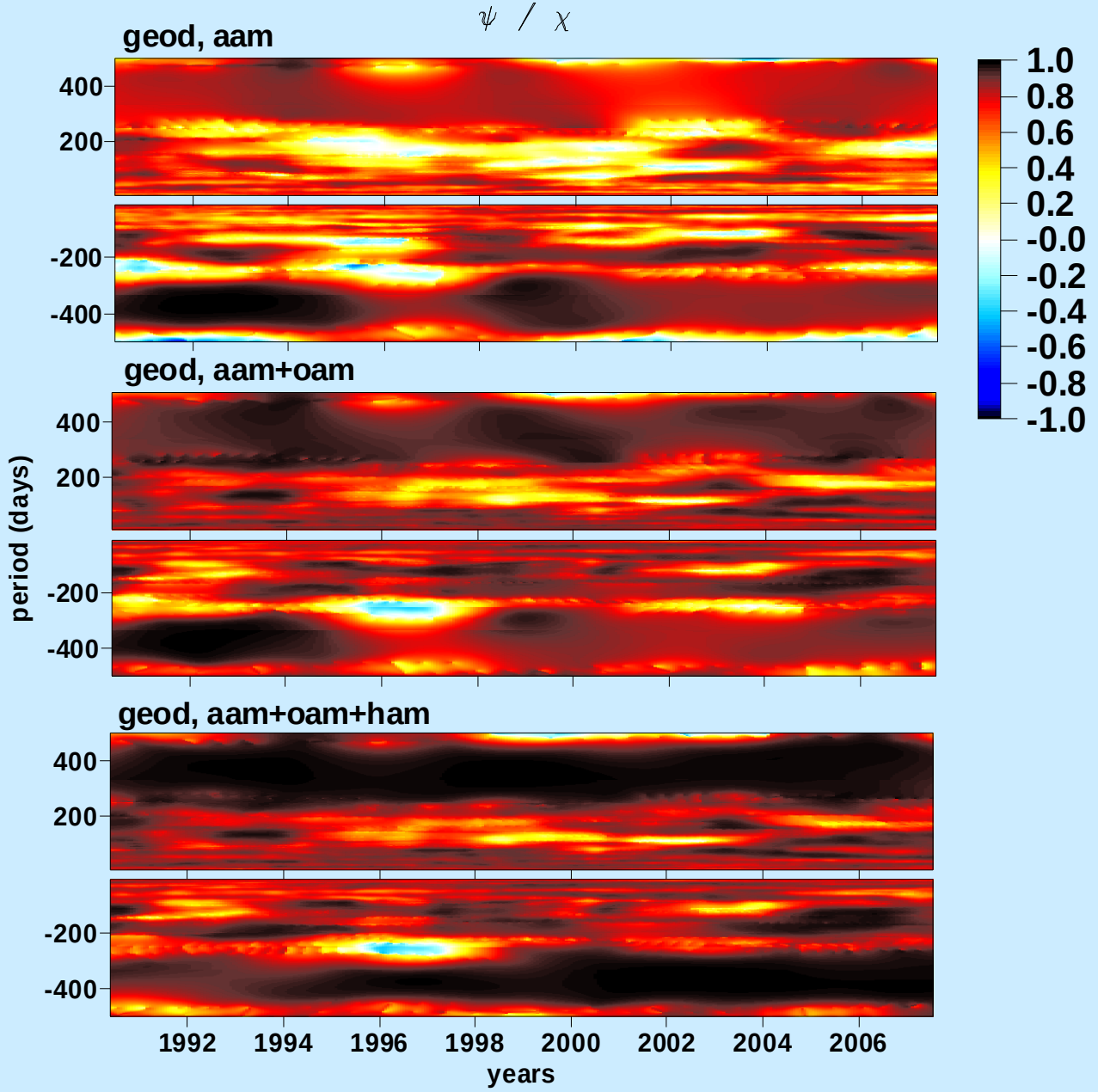

The common oscillations in the equatorial components of geodetic (black) and AAM, AAM+OAM and AAM+OAM+HAM excitation functions, computed using wavelet based semblance filtering (threshold equal to 0.9).